

Adaptive Kernel Density Estimation proposal in gravitational wave data analysis

Mikel Falxa,¹ Stanislav Babak,¹ and Maude Le Jeune¹

¹*Université Paris Cité, CNRS, Astroparticule et Cosmologie, F-75013 Paris, France*

(Dated: September 2021)

Markov Chain Monte Carlo approach is frequently used within Bayesian framework to sample the target posterior distribution. Its efficiency strongly depends on the proposal used to build the chain. The best jump proposal is the one that closely resembles the unknown target distribution, therefore we suggest an adaptive proposal based on Kernel Density Estimation (KDE). We group parameters of the model according to their correlation and build KDE based on the already accepted points for each group. We adapt the KDE-based proposal until it stabilizes. We argue that such a proposal could be helpful in applications where the data volume is increasing and in the hyper-model sampling. We tested it on several astrophysical datasets (IPTA and LISA) and have shown that in some cases KDE-based proposal also helps to reduce the autocorrelation length of the chains. The efficiency of this proposal is reduced in case of the strong correlations between a large group of parameters.

I. INTRODUCTION

We live in the era of large physics and astrophysics projects and often have to deal with large and complex datasets. The data analysis usually requires large computing facilities and a single computation could sometimes last for weeks. Optimizing the analysis techniques and pipelines is then a key challenge of the data science associated with all large (astro)physical experiments.

Nowadays, it is quite common to use Bayesian framework for analysing the data. It is especially convenient if we have a parameterized data model (or several competing models) describing the data. In this approach we treat all parameters as random variables with some prior based either on some physical principles or informed from the previous independent experiments. We use the observations at hands to refine our prior knowledge and infer a posterior probability distribution function for parameters of a model, or even perform a selection among several models. Often we have to deal with multidimensional parameter space with a non-trivial likelihood function which can be evaluated only numerically. One of the most used tool to perform the numerical sampling from a target distribution is Markov Chain Monte Carlo (MCMC). Building a Markov chain that represents the desired posterior requires two key ingredients: (i) proposal suggesting how to choose point \vec{X}_{i+1} given the last point in the chain \vec{X}_i ; (ii) the detailed balance which ensures the reversibility of the chain. One of the most successful and frequently used proposal approach is to use parallel tempering: running several chains with logarithmic distributed temperature ladder (see for example [4]). The hot chains play role of a proposal there and its efficiency depends on the interplay of number (and distribution) of hot chains (more chains is better) and computational demands (increase with the number of chains). Understanding the properties of the signal and the likelihood surface often leads to a custom proposal suitable for a particular problem.

Here we suggest another generic proposal based on the Kernel Density Estimation (KDE). The idea of using KDE is not new and might seem a rather trivial. The main result of this paper is in a particular implementation of KDE itself and its embedding into a sampler. Even though the proposed method

is very generic we will mainly discuss its implementations in the gravitational waves (GWs) data analysis.

Let us summarize the key points of the KDE-based proposal.

- KDE is used together with the set of other proposals in building a Markov chain. We assume an adaptive approach where we use the data accumulated in a chain to regularly rebuild the KDE. We repeat adjustments until the convergence criteria based on the Kulback-Leibler divergence is satisfied.
- In order to build KDE we split all parameters into several groups, where parameters in each group show evidence of mutual correlation. The KDE-based proposal is most efficient if the full parameter space could be split into many small uncorrelated groups. The performance drops significantly if dimensionality of a group is larger than 5.
- We have build KDE with the self-optimizing bandwidth based on the distribution of a sample points provided at the input.

Note that the adaptation breaks “Markovian” properties of the chain. Either one should dismiss the parts of the chain during the adaptation or, in case of uninterrupted adaptation, assume that the chain is only asymptotically Markov. We give detailed description of implementation in the next two sections (II, III).

We have implemented the KDE-based proposal in a particular sampler <https://gitlab.in2p3.fr/lisa-apc/mc3>. We give a detailed description of this sampler in Appendix C. The main feature of this sampler is that it runs several chains either completely independently or as parallel tempering. Multi-chain run is used to compute Gelman-Rubin ratio [9] to monitor the convergence.

We assess the performance of the suggested proposal in two applications to GW data analysis. In first one we analyse the data combined by International Pulsar Timing Array (IPTA) collaboration searching for a continuous GW signal in the nano-Hz band. As the second dataset we use simulated LISA data publically available through LISA Data Challenge

(2a) portal. We use the KDE-based proposal to infer parameters of 6 Galactic white dwarf binaries. We present the performance of our proposal for those two data analysis problems in Section IV, in particular we show that the KDE-based proposal allows to reduce the autocorrelation length while keeping high acceptance rate.

We conclude the paper with discussion on the limitation and possible extension of our method in Section V.

II. KERNEL DENSITY ESTIMATION

In this rather short section we describe our particular way of building KDE. We start with a short introduction to KDE and then give details of the bandwidth optimization that we use.

A. Brief introduction

KDE is a non-parametric method used to estimate a probability density function (pdf) based on a finite set of sample points [21][24]. It is a smooth alternative to a histogram. The advantage of KDE is that it uses no binning and gives a continuous function interpolating (and extrapolating) across the whole parameter space. For a d -dimensional dataset $\{\vec{X}\}$ of size N and kernel $K(\mathbf{x}, \vec{h})$, we have our KDE $\hat{f}(\mathbf{x}, \vec{h})$:

$$\hat{f}(\mathbf{x}, \vec{h}) = \frac{1}{N} \sum_{a=0}^{N-1} K(\mathbf{x} - \vec{X}_a, \vec{h}), \quad (2.1)$$

with parameter \vec{h} specifying the bandwidth of the kernel. We use latin subscripts from the first half of the alphabet to enumerate the samples in the set. The main idea is to sum smooth kernel functions of \mathbf{x} centered on each sample (input) data point \vec{X}_a . The overlaps between neighbouring kernels will add-up, shaping the PDF for the set of samples $\{\vec{X}\}$. The choice of the kernel is arbitrary and we choose to work with a gaussian kernel of the form:

$$K_g(\mathbf{x} - \vec{X}_a, \vec{h}) = \prod_{i=1}^d \frac{\exp\left\{-\frac{1}{2} \frac{|\mathbf{x} - \vec{X}_{a,i}|^2}{h_i^2}\right\}}{\sqrt{2\pi}h_i}, \quad (2.2)$$

where the h_i is the local bandwidth corresponding to i -th parameter $|\mathbf{x} - \vec{X}_{a,i}|$, and d is the dimensionality of the parameter space. We use the latin letter from the second half of the alphabet to enumerate particular parameters, and the vector notation corresponds to a vector in the parameter space.

B. Optimal bandwidth

A KDE has one free parameter which we want to tune, the bandwidth \vec{h} . Its value should be adapted to the dataset we are

working with. There is no direct way of estimating it and we use an optimisation method [15] based on the minimisation of the mean squared error (MSE) ϵ^2 with respect to \vec{h} :

$$\epsilon^2 = \int d\mathbf{x} (\hat{f}(\mathbf{x}, \vec{h}) - f(\mathbf{x}))^2, \quad (2.3)$$

$$\frac{\partial \epsilon^2}{\partial \vec{h}} = 0, \quad (2.4)$$

where $f(\mathbf{x})$ is the true pdf that we want to approximate with the KDE. The numerical way of evaluating this integral is given in the appendix B.

Instead of using a global bandwidth \vec{h} , we can define a local bandwidth \vec{h}_a for each kernel $K(\mathbf{x} - \vec{X}_a, \vec{h}_a)$ [28]. In that case, our KDE $\hat{f}(\mathbf{x}, \vec{h})$ is:

$$\hat{f}(\mathbf{x}, \vec{h}) = \frac{1}{N} \sum_{a=0}^{N-1} K(\mathbf{x} - \vec{X}_a, \vec{h}_a). \quad (2.5)$$

Intuitively we expect the local bandwidth \vec{h}_a to be scaled according to the local density of points. Indeed, the bandwidth is chosen so that it is narrow in the regions of parameter space where the samples are most dense and it is broad where we have fewer samples. This can ensure good interpolation and overlap between kernels, in particular, in high dimensional problem where the sample points are very sparse.

In practice we use solution of equation 2.4 to find optimal local bandwidth. The global bandwidth (if needed) could be defined as an average over all local values (by setting the input parameter `global bw = True`).

In Appendix B, we have shown that each local bandwidth $\vec{h}_a = [h_{a,1} h_{a,2} \dots]$ of the kernel centered on point \vec{X}_a can be approximated by solving a linear system for the k nearest neighbours \vec{X}_b of the form:

$$\mathbf{A}(\vec{X}_b) \begin{bmatrix} \frac{1}{h_{a,1}^2} \\ \frac{1}{h_{a,2}^2} \\ \vdots \end{bmatrix} = \vec{B}(k) \quad (2.6)$$

Matrix \mathbf{A} and vector \vec{B} are given in Appendix B eqn. B6, where we provide a detailed description of the method. They depend on the position of nearest neighbours which are the k_{near} points contained in a hypercube centered on the point \vec{X}_a in the parameter space. The edge ΔX_i of the hypercube for each parameter X_i is defined as:

$$\Delta X_i = (\max_{\{\vec{X}\}} X_i - \min_{\{\vec{X}\}} X_i) / s \quad (2.7)$$

where maximisation and minimisation are performed over the set of input samples and s is a scaling parameter we call "adapt scale".

It might happen that a hypercube contains no point (besides the central). In that case, we cannot compute the local bandwidth and the point is discarded. Its bandwidth is later set to the global bandwidth as defined above. In case of high dimensionality and if the points in the dataset are very sparse, we change parameter s iteratively decreasing by a factor 2 until we find non-empty hypercubes. However, if this happens the evaluation of the bandwidth will probably be flawed and there is not much we can do about it, except use bigger datasets with more sample points. Often the amount of additional points that is needed to cover all “holes” could be very large incurring unmanageable computational cost. That is why good parameter grouping is essential : reducing dimensionality without loss of correlated features in the data. This will be the main subject of the next section.

III. METHOD

The main idea is to build a KDE for a given d-dimensional set of sample points $\{\vec{X}\}$. However, for a high dimensional KDE we are strongly affected by the “curse of dimensionality” [25] because the sample sets are often limited in size leaving under-covered regions of the parameter space. In addition the efficiency of KDE is degrading if there are too many points since we place the kernel on top of each sample. For that reason, we will split a d-dimensional parameter space into several low dimensional subspaces grouping the most correlated parameters together. We assume that sub-groups are not correlated and build the KDE for each of them $\hat{f}_\alpha(\mathbf{x}_\alpha, \vec{h}_\alpha)$, so the total KDE is the product of the low-dimensional KDEs:

$$\hat{F}(\mathbf{x}, \vec{h}) = \prod_{\alpha} \hat{f}_\alpha(\mathbf{x}_\alpha, \vec{h}_\alpha), \quad (3.1)$$

where the greek indices enumerate the subgroups of parameters. Forming these subgroups relies on the assessment of the correlation between parameters based on the provided set of samples $\{\vec{X}\}$ and this is the main subject of the next subsection.

A. Parameter grouping

For a d-dimensional dataset $\{\vec{X}\}$ we want to split the parameters in several sub-groups. Each sub-group will contain correlated parameters while parameters from different sub-groups will be uncorrelated. We could use a covariance matrix to identify correlations, however it implicitly assumes Gaussian distribution and cannot account for any complex 2D structures between pairs of parameters. Instead we use a method based on the Jensen-Shannon divergence (JSD) [20]. JSD, similarly to the Kullback–Leibler (KL) divergence, measures the similarity between two distributions, but with the advantage of being symmetric and bound $0 \leq JSD \leq \ln 2$, moreover it does not make any assumptions about the distributions. For each pair of parameter (X_i, X_j) with the joined probability distribution $p(X_i, X_j)$ we compute

$$0 \leq JSD(p(X_i, X_j) \| p(X_i)p(X_j)) \leq \ln 2, \quad (3.2)$$

where the second distribution $p(X_i)p(X_j)$ is a product of one-dimensional (marginalized) distributions obtained by shuffling the parameters $\{X_i, X_j\}$ that supposed to destroy any correlations between parameters X_i, X_j (see figure 1). If the JSD is low, it means that the shuffling did not affect the dataset and the parameters did not exhibit correlation. On the other hand, if the JSD is large, the shuffling did change something and the parameters should be grouped together.

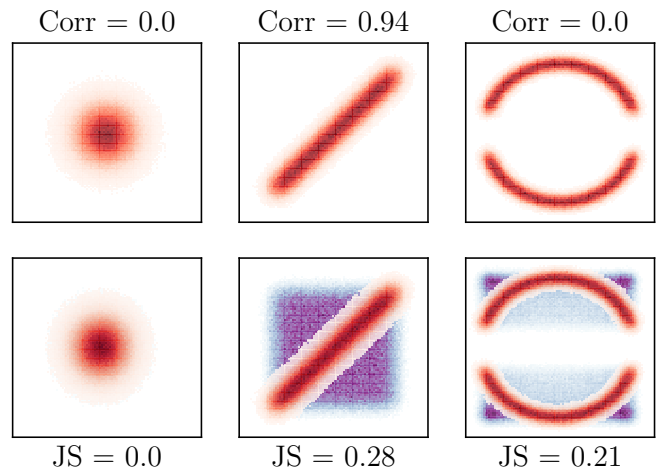


FIG. 1. We plot three examples of datasets where we have on the left no correlation, in the middle linear correlation and on the right more elaborate features. On the top panels we have the corresponding values of the correlation coefficient based on simple evaluation of the covariance matrix. We see that it excels at finding the linear correlation but completely fails with the right panel features. On the bottom panels we have the same three datasets in red with their corresponding shuffled version that destroys correlations in blue. While the left panel remains unchanged, the others are affected and it is captured by the JS divergence.

We define a JSD threshold (we usually use 0.1) which we consider that two parameters are correlated. Starting from one parameter, we iterate the process to extract all correlated (chained) pairs. Once no additional correlated parameter is found, we take the union of all correlated pairs of parameters to form a sub-group. This process is illustrated in figure 2.

In case of multimodality of the probability distribution function that we try to reproduce with KDE, we implemented an additional (optional) feature: clustering samples before building KDE. This feature is especially welcome when the modes are separated by very low probability valleys. We cluster the samples (using k-means method [18]) and apply KDE building approach described above to each mode. This does not change the fundamental structure of the KDE but it helps the bandwidth adaptation.

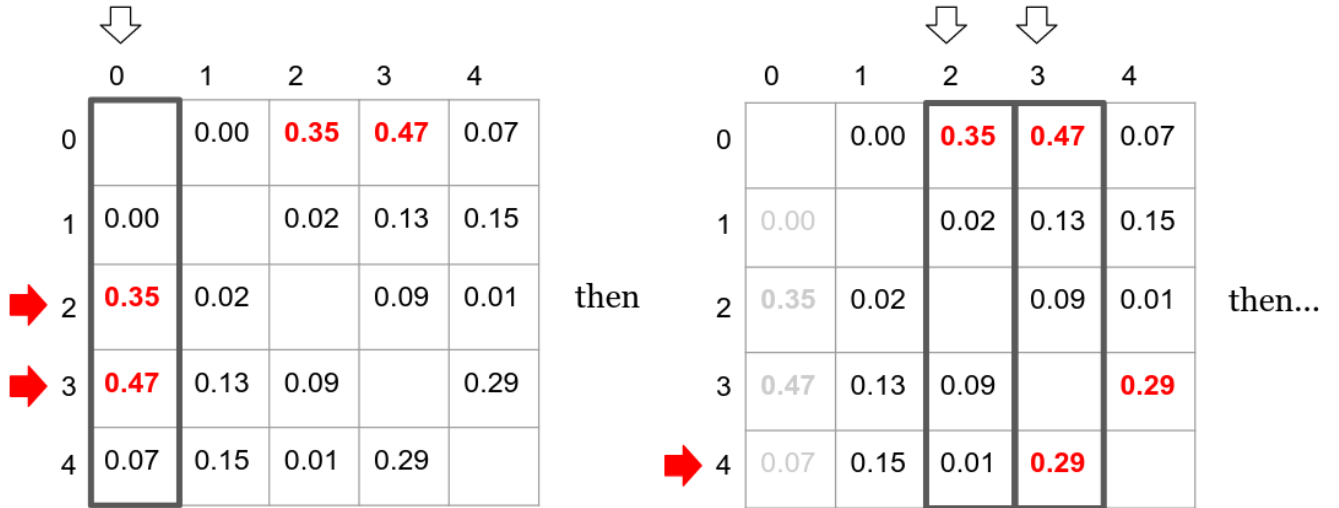


FIG. 2. Illustration of the parameter grouping process using a JSD matrix. For this example, the JSD threshold is set to 0.25, hence the parameter sub-groups will be [0, 2, 3, 4] and [1]. Starting from parameter 0, we find that JSD for parameters 2 and 3 are above the threshold so they are both correlated with parameter 0. Then we check for parameters 2 and 3 and find that 4 is correlated with 3 while 2 sees no additional correlation. The last step would have been to check for 4 and find that there are no additional correlations. Therefore, 0, 2, 3 and 4 will form a sub-group of correlated parameters. The parameter “1” is the last parameter that does not correlate with others (according to the adopted threshold) and it will be a sub-group on its own.

B. KDE: turning posterior into proposal

It is desirable in several application to use posterior points inferred for some parameters into a prior for another investigation. Let us give several examples:

- The data inferred from electromagnetic observations in form of samples is used as a prior for the GW experiment. In this case we can either build a joined likelihood or, alternatively, build KDE on the external posteriors and use it as a prior while analyzing the GW data.
- In Pulsar Timing Array (PTA) data analysis we often first investigate data acquired for each pulsar and trying to build a noise model. Later this pulsar and associated noise model is plugged into “Array” of pulsars for searching for a GW signal. It is proven to boost significantly efficiency of the GW search if we use posteriors for the noise model inferred in the first step as a proposal in the global fit later on.
- Often the data is taken continuously and we want to analyse it “on the fly”; that is true for GW data analysis. In this case you want to increment the data with a certain cadence while using information about the sources acquired from the analysis of the past data. One possibility is to turn again posterior built from the analysis of, say, first half a year of data into a prior in the analysis of the whole year of data.
- The method in [12] gives a practical suggestion on how to compute the Bayes factor comparing several models without computing the evidence for each model. In this

approach we introduce hyper-parameter indexing the models and jump in this parameter (say, within MCMC) which corresponds to jumping between the models. For this method to be robust the exploration within each model must be very efficient otherwise it will lead to very long poorly converging runs or to spurious results. If we have posteriors for each (or some) model available, we can turn them into proposal and use in the hyper-model exploration.

The main idea of grouping parameters in building KDE implies that we probably also want to make jumps within each subgroup (or in some subgroups) while keeping other parameters fixed (Gibbs-like sampling). The subgroups for a current jump are chosen randomly assuming equal probability attached to each subgroup. The randomness implies reversibility and equal probability is a warrant that we jump in all parameters evenly (on average) while performing low dimensional jumps. Let us denote the number of sub-KDEs that is used for each jump n_{kde} , then the proposal probability is

$$\hat{F}_{n_{kde}}(\mathbf{x}, \vec{h}) = \prod_{\alpha}^{n_{kde}} \hat{f}_{\alpha}(\mathbf{x}_{\alpha}, \vec{h}_{\alpha}), \quad (3.3)$$

where the subscript in \mathbf{x}_{α} implies that we vary only parameters that belong to that (α) subgroup. This probability is used to balance the chain in the Metropolis-Hastings step of the MCMC algorithm [11]. Choosing a point from a given sub-KDE $\hat{f}_{\alpha}(\mathbf{x}_{\alpha}, \vec{h}_{\alpha})$ is done by drawing a point from the randomly chosen kernel $K(\mathbf{x} - \vec{X}_{\alpha}, h_{\alpha})$ of $\hat{f}_{\alpha}(\mathbf{x}_{\alpha}, \vec{h}_{\alpha})$ centered on \vec{X}_{α} :

$$\vec{X}_b^* \rightarrow \vec{X}_a + \mathcal{N}(\vec{0}, h_a), \quad (3.4)$$

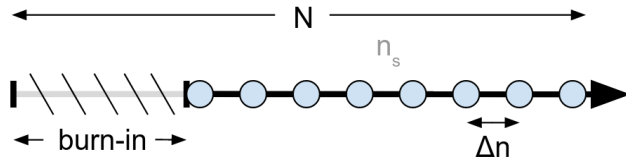


FIG. 3. For a chain of total length N , we get rid of the burn-in, then we extract n_s linearly spaced samples from the remaining fraction of the chain. These n_s points are used to build the KDE.

where $\mathcal{N}(\vec{0}, h_a)$ is a normally distributed random variable with $\vec{0}$ mean and covariance matrix $\text{diag}(h_a)$ that is the bandwidth of kernel $K(\mathbf{x} - \vec{X}_a, h_a)$. For a random set of n_{kde} sub-KDEs, the newly proposed point \vec{X}^* is the union of parameters from each subgroup \vec{X}_b^* :

$$\vec{X}^* = \bigcup_b \vec{X}_b^*. \quad (3.5)$$

C. Adaptive proposal

In case we do not have samples from the previous investigations, we still can build KDE-based proposal using the points accepted by a running MCMC. There are several caveats which need to be considered: (i) during the burn-in and even some time after the distribution of the accepted points is quite unstable that will reflect on the KDE (ii) we are breaking the rules of MCMC, the chain is only asymptotically Markov, so that at some point we should fix the KDE-based proposal and dismiss all samples accumulated before. The rest of this subsection gives the details of the practical implementation of the adaptation.

To build a KDE on the currently sampled chain, we select only a subset of the total N samples. In particular, we take n_s uniformly spaced points, from burn-in to the last point, as illustrated in Figure 3. The burn-in is taken to be a fraction, q , of the total chain length N and those points are dismissed (hence, $n_s = (1 - q)N$). As chain evolves, the burn-in could also grow until we get to the stationary distribution. The post-burn-in length is also increasing, and, since we keep n_s fixed, the space Δn between the selected samples grows. We expect that the quality of the KDE improves with increase in Δn because of the reduced correlation in the samples taken for building KDE, and that is true until Δn reaches typical autocorrelation length of the chain [13].

We re-build a new KDE after each N_{adapt} iterations (jumps) of the chain. We want to track the evolution of KDE and stop adapting when it has reached stability (that could be another indicator of the burn-in phase). We compare the new (re-built) KDE $\hat{F}_1(\mathbf{x}, \vec{h}_1)$ with the old $\hat{F}_0(\mathbf{x}, \vec{h}_0)$ by computing the KL divergence [16]:

$$\text{KL}(\hat{F}_0 \parallel \hat{F}_1) = \int d\mathbf{x} \hat{F}_0(\mathbf{x}) (\log \hat{F}_0(\mathbf{x}) - \log \hat{F}_1(\mathbf{x})) \quad (3.6)$$

This integral could be approximated as

$$\text{KL}(\hat{F}_0 \parallel \hat{F}_1) \approx \frac{1}{n_s} \sum_a (\log \hat{F}_0(\vec{X}_{0a}, \vec{h}_0) - \log \hat{F}_1(\vec{X}_{0a}, \vec{h}_1)), \quad (3.7)$$

where $\{\vec{X}_0\}$ is the set of n_s samples used to build $\hat{F}_0(\mathbf{x}, \vec{h}_0)$. This gives a measure of change in KDE between successive updates: ΔKL . We stop updating KDE in order to preserve the ergodicity of the process [2] as soon as convergence criterion

$$\frac{|\langle \Delta \text{KL} \rangle|}{\sqrt{\langle \text{KL}^2 \rangle}} < 5\% \quad (3.8)$$

is satisfied. The angular brackets denote the averaging over the last 5 updates and we demand that the average change in KL is small compared to the average KL values. ΔKL can be negative or positive, depending on the evolution of KL. If KL does not converge to a specific value, this condition ensures that it is at least oscillating around a mean value.

IV. RESULTS

We consider two datasets and perform search/parameter estimation using MCMC with KDE-based proposal.

In first application we consider a dataset from International PTA collaboration and perform the noise analysis for each pulsar in the array [22]. The likelihood is expected to be quite broad and unimodal but the dimensionality of the parameter space is large as well as its overall volume.

In second application we work with the simulated LISA data and search/characterize small bandwidth with several Galactic white-dwarf binaries. The likelihood in this case has more complex structure with quite strong correlation between parameters.

We quantify performance of the KDE-based proposal using the following criteria:

- Closeness between built KDE and the true distribution using **KL divergence**¹.
- The **acceptance rate** when the KDE is used as a proposal with MCMC sampler
- The **autocorrelation length** [13] of the MCMC chain when the KDE is used as proposal, to evaluate improvement in the mixing of the chain.

¹ Because we do not know the true distribution, we have to use histograms to evaluate KL. The formula for binned KL is given in Appendix A.

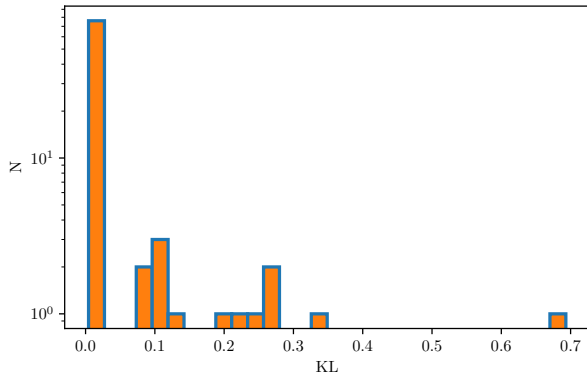


FIG. 4. Distribution of the KL divergence for all sub-KDEs. 1-d sub-KDEs are of best quality.

A. IPTA dataset

We build the KDE using $n_s = 10000$ samples from the chains generated by previous MCMC runs. We adopt the following choice of parameters for generating KDE:

- js threshold = 0.1
- adapt scale = 10
- use kmeans = False
- global bw = True
- n kde = 1

Within total 104 parameters, the grouping algorithm finds : **76** 1-dimensional sub-groups, **12** 2-dimensional sub-groups and **1** 4-dimensional sub-group. For each of these sub-groups we calculate the KL divergence $KL(p_\alpha(\mathbf{x}_\alpha) \parallel \hat{f}_\alpha(\mathbf{x}_\alpha, \vec{h}_\alpha))$ of the true pdf of the subgroup $p_\alpha(\mathbf{x}_\alpha)$ against the corresponding sub-KDE $\hat{f}_\alpha(\mathbf{x}_\alpha, \vec{h}_\alpha)$. A good sub-KDE should give a $KL(p_\alpha(\mathbf{x}_\alpha) \parallel \hat{f}_\alpha(\mathbf{x}_\alpha, \vec{h}_\alpha))$ that is close to 0. Because the number of parameter is large, we show the histogram plot in figure 4 depicting KL for each subgroup.

The impact of the dimensionality of the sub-KDE on KL can be clearly seen in Figure 4. Close to 0 we have 76 1-dimensional sub-KDEs, between 0.1 and 0.4 we have 12 2-dimensional sub-KDEs, and the 4-dimensional sub-KDE has $KL \approx 0.7$. As discussed in the previous section, increasing dimensionality implies sparse data samples, so we expect KL values to rise because the KDE might fail to interpolate the PDF correctly between neighbouring points, producing holes in the distribution. Computing KL allows us to quantify this effect and assess the quality of the KDE that may not be obvious by just eyeballing (see figure 5).

Next we will analyse the IPTA data using MCMC sampler [6] and ENTERPRISE [7] package for computing likelihood function. We chose to use two jump proposals Single-Component Adaptive Metropolis (SCAM) [10] and Differential Evolution (DE) [14, 27] to compare to KDE. We search for

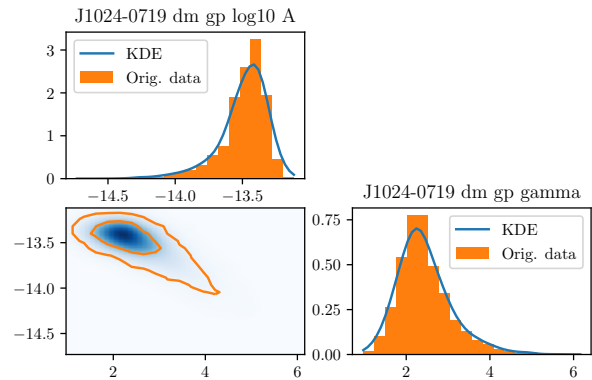


FIG. 5. 2-dimensional corner plot of binned original dataset against smooth KDE plot. KDE is blue, original is orange. The contour levels for the original dataset on the bottom left panel are [0.1, 0.95]. For this sub-KDE, $KL \approx 0.11$.

	KDE	SCAM	DE
Acceptance rate	0.57	0.39	0.43

TABLE I. Acceptance for various proposals (KDE run)

a continuous gravitational wave signal while fitting for pulsar noise parameters [1]. The KDE for the noise parameters has been built using posterior samples obtained from the preceding single pulsar analysis. We will compare three different runs:

- using a KDE-based + default jump proposals SCAM and DE (labeled as “KDE”);
- using binned empirical distributions + default proposals SCAM and DE (labeled as “Binned”);
- using only default proposals SCAM and DE (labeled as “None”).

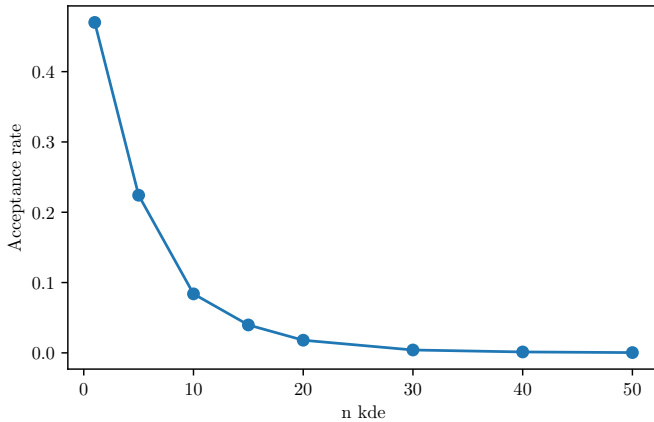
The binned empirical distributions are essentially 2-dimensional histograms based on the same posterior samples as used in building KDE [26]. Those carry a similar spirit to KDE, being pair-wise approximation to marginalized posterior, but at the same time are fundamentally different from the KDE in the sense that the KDE is a continuous function in space that interpolates between the sample points using smoothing kernel. In addition KDE-based proposal makes grouping based on the parameter correlation that could lead to more than two dimensional group (see figure 4).

Tables I, II, compare acceptance rate of different proposals in two independent runs. One can see that KDE has the highest acceptance rate due to smart parameter grouping and interpolation between the samples incorporated in the KDE-based

	Binned	SCAM	DE
Acceptance rate	0.47	0.41	0.43

TABLE II. Acceptance for various proposals (binned proposal run)

n_{kde}	KDE	SCAM	DE
1	0.47	0.41	0.43
5	0.22	0.36	0.41
10	0.08	0.35	0.40

TABLE III. Acceptance for different n_{kde} FIG. 6. Acceptance rate for several values of n_{kde} .

proposal. For the jumps we could use simultaneous jump in one or several (n_{kde}) sub-groups. Increasing n_{kde} leads to the higher dimensionality of the jumps and has a strong impact on the acceptance rate as shown in Figure 6. The best results are achieved if we perform jumps in one subgroup at the time, the acceptance rate decreases exponentially with n_{kde} .

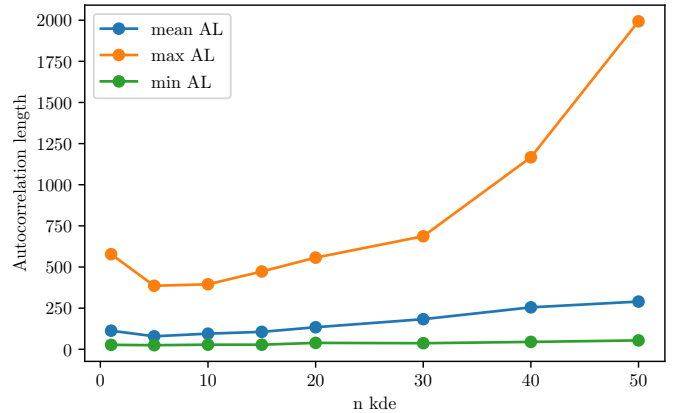
A high acceptance rate is not necessarily a sign of a good proposal as it has to be paired with the low autocorrelation length. For each run, we compute the autocorrelation lengths of all parameters and compare the maximum, minimum and mean autocorrelation lengths. The low autocorrelation length implies that the samples drawn/accepted are independent. Results are presented in Table IV. KDE performs very well for IPTA data. Minimum autocorrelation length does not seem to be affected much by the choice of proposal but the maximum is reduced by a factor 2 when using KDE. Reducing the maximum is the most important because thinning the chain by this factor ensures that all samples are independent for all parameters. The mean autocorrelation length is just an indicator of the average performance of the proposal.

Like for the acceptance rate, we check the influence of n_{kde} on the autocorrelation length. Results are given in Table V. For high values of n_{kde} , even though we have decreasing acceptance rate, the autocorrelation drops too and mixing improves. However, this result should be take with a caution,

	max	min	mean
KDE	578	27	113
Binned	1386	29	160
None	1032	25	208

TABLE IV. The maximum, minimum and mean autocorrelation lengths for three runs.

n_{kde}	max	min	mean
1	578	27	113
5	386	25	79
10	395	28	95

TABLE V. The maximum, minimum and mean autocorrelation lengths for different n_{kde} .FIG. 7. Mean, maximum and minimum autocorrelation lengths for several values of n_{kde} .

using high n_{kde} could lead to a very low acceptance point as shown in Figure 6. In Figure 7 we show the autocorrelation length as a function of n_{kde} and it indicates that the optimal number is around $n_{kde} = 5$ with acceptance rate of 0.22 that is very close to the expected optimal acceptance rate of 0.234 [8]. Based on these results, we recommended to work with values of n_{kde} between 1 and 10, especially when the dimensionality of the parameter space is high like in this IPTA example.

B. LISA dataset

Now we turn our attention to the simulated LISA data, in particular, we use “Sangria” dataset which is 1 year long, it contains about a dozen of merging massive black hole binaries and about 30 millions of Galactic binaries <https://lisa-ldc.lal.in2p3.fr/>. Here we are interested in Galactic binaries in the very narrow frequency range around 4 mHz and we have removed all merging black holes. We have detected 6 sources in that frequency interval and we use KDE-based proposal together SCAM and DE². This time we use home-made sampler *M3C2* <https://gitlab.in2p3.fr/lisa-apc/mc3>, specifically parallel tempering version of it. We describe this sample in details in the Appendix C. This sampler is using Metropolis-Hastings acceptance-rejection step as well as *slice* sampling [19].

² The DE introduced in [27] is using population MCMC, here we rather use it on a single chain in the spirit described in the snooker proposal in [14]

Each Galactic binary is characterized by 8 parameters, so we have in total 48 parameters [17]. We expect some parameters (like amplitude and the orbital inclination angle) to correlate for each source, and, in addition, some parameters could correlate between the sources. Here we try to build a proposal on-the-fly. The likelihood surface for this problem is rather complex having many well separated maxima (reason for using parallel tempering). We will build KDE as we accumulate samples: adapting KDE proposal with the rate every 5000 samples and using $n_s = 5000$ samples for each chain. Besides KDE we also use SCAM proposal and slice sampling. Note that the combination of SCAM jump with Metropolis-Hastings sampling and slice (being very independent) already significantly reduce the autocorrelation of the accepted points.

First, we consider the convergence of KDE adaptation. During the burn-in stage the KDE is changing quite violently. The correlation between parameters is quite unstable which leads to fluctuation in how parameters are grouped and in the number of subgroups. As burn-in proceeds we keep track of the grouping and fix the splitting in sub-groups as soon as it stabilizes (when the same grouping appears at least 5 times). Once we have fixed sub-groups we check the KL divergence between the subsequent updates of KDE (as described above). The results of KDE adaptation are presented in Figure 8. The consistent grouping of parameters was reached after 26 updates as indicated by a dashed red line. Then we compute KL after each update and stop adaptation once the condition 3.8 is met (see the right panel of Figure 8). From then on we keep KDE fixed and perform the actual sampling.

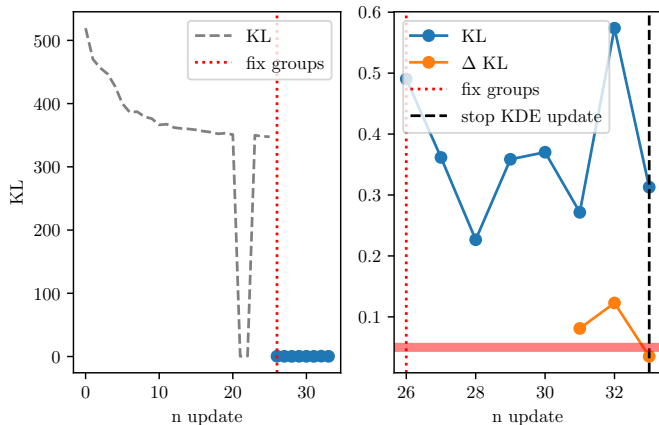


FIG. 8. Evolution of KL and Δ KL. Left panel, evolution of KL before fixing parameter groups. Right panel, evolution of KL after fixing parameter groups, we start computing Δ KL 5 updates after the grouping was fixed. The thick red line indicates the Δ KL threshold level of 5% below which we reach convergence.

As a next step we want to check the acceptance rate of the KDE-based proposal and compare it to SCAM and slice. Note that slice is not based on the Metropolis-Hastings acceptance/rejection algorithm, however we still can introduce an effective acceptance rate as a ratio of total number of slice calls to the total number of likelihood evaluations used by slice.

We consider two cases for the subgroup jumps $n_{kde} = 1$ and $n_{kde} = 5$. Figure 9 compares acceptance rate for $n_{kde} = 1$. One can see that it stabilizes around 0.31 very fast, and, despite that it is lower than what we had for the PTA application, it is a very decent acceptance rate. SCAM has a similar acceptance (but usually longer autocorrelation length), while slice is worse by a factor 10 (though it usually has low autocorrelation length).

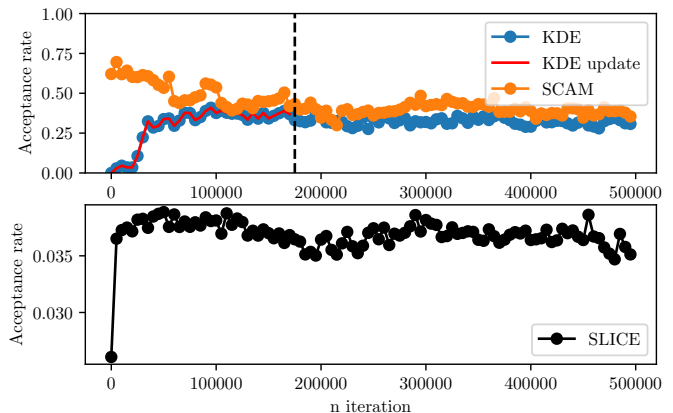


FIG. 9. Acceptance rate of all proposals for $n_{kde} = 1$. KDE and SCAM are on top panel, SLICE on bottom panel. Red plot and black dashed line shows where KDE finally converged and stopped updating.

Figure 10 compares acceptance rate for $n_{kde} = 5$. Increase in the dimensionality of the jumps has a drastic effect on the acceptance rate, its value drops to about 0.015. It is also interesting to compare behaviour of SCAM and slice for two runs. Slice shows very stable/consistent results, while SCAM has significant fluctuations though preserving the trend. The two-dimensional KDE jumps seem to be the best option in this application.

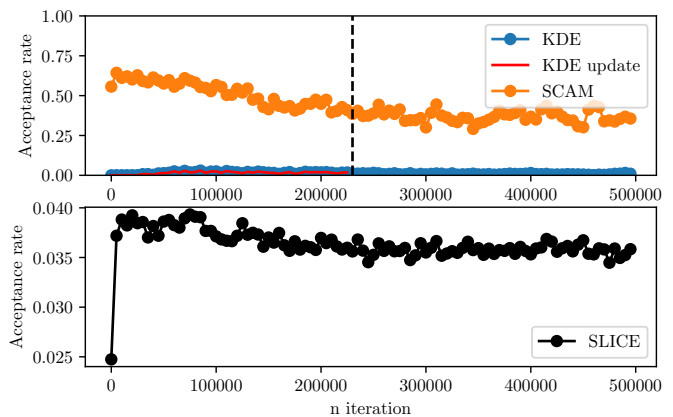


FIG. 10. Acceptance rate of all proposals for $n_{kde} = 5$. KDE and SCAM are on top panel, SLICE on bottom panel. Red plot and black dashed line shows where KDE finally converged and stopped updating.

Next we check the autocorrelation length when we run with

and without KDE-based proposal. We restrict ourselves with the case $n_{kde} = 1$ since $n_{kde} = 5$ has a very poor acceptance rate. Figure 11 compares maximum and mean autocorrelation of two runs. We observe that the mean value is slightly (about 17%) lower when we include KDE-based proposal and the maximum length remains the same. As we have already mentioned, mixing SCAM with Metropolis-Hastings and slice steps does reduce the autocorrelation already (compared to PTA example where we did not use slice sampling). In addition we use parallel tempering algorithm, where the hot chains could be seen as yet another jump proposal. All in all, KDE does not add much to already reduced autocorrelation run in the current analysis.

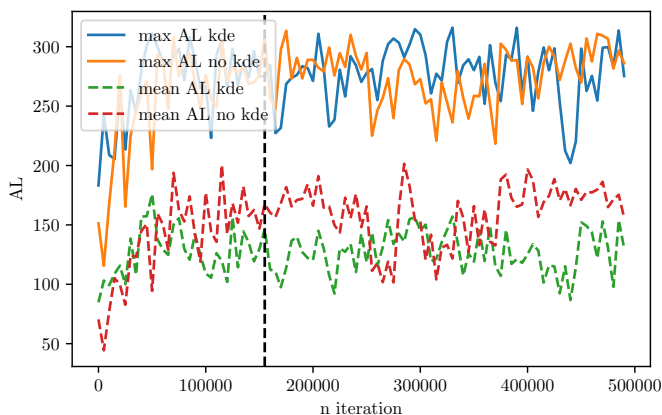


FIG. 11. Maximum and mean autocorrelation lengths for $n_{kde} = 1$, comparing a run with KDE against a run without KDE. Black dashed line shows where KDE finally converged and stopped updating.

V. CONCLUSION

Bayesian formalism is a usual approach in nowadays gravitational waves data analysis. The inference of the parameters posterior distribution is often done using MCMC and the efficiency strongly depends on the proposal it uses. In this article we have presented KDE-based proposal which can be either built on-the-fly during the extended burn-in stage or constructed using posterior points from another run.

The suggested KDE-based proposal has several extended features: (i) the adaptive bandwidth based on the local density of points (small bandwidth in the densely sampled regions of the parameter space); (ii) splitting parameter space into subgroups of the correlated parameters and applying KDE on each subgroup, we identify correlations using JSD; (iii) possibility of building KDE adaptively.

We tested this proposal by running MCMC on IPTA data, using a KDE that we have built from previous MCMC runs (i.e. non adaptive case). The advantage of KDE-based proposal was clearly seen in high acceptance rate with low autocorrelation length. We have found that using rather low value $n_{kde} = 1 - 5$ (number of subgroups used in the jump simultaneously) seems to be optimal.

Another application of the KDE-based proposal was in running PTMCMC on the simulated LISA data searching for Galactic white dwarf binaries in a narrow frequency band. In this case we have built KDE adaptively during an extended burn-in stage. The addition of KDE-proposal to the sampling had only a moderate impact: it shows a decent acceptance rate (about 31%) with only small improvement in the autocorrelation length. Moreover we have shown that low-dimensional jumps are strongly preferred.

Few things could be improved, most notably in the adaptation. The threshold for grouping parameters was chosen somewhat ad hoc, and correlation of some parameters could be close to the threshold. We did observe the fluctuation in choosing the subgroups during the adaptation. One possibility could be to choose not one but two plausible grouping, build KDE for each and use two KDE proposals in a probabilistic manner. The criteria for stopping adaptation was also chosen somewhat arbitrary, and might benefit from the further tuning. Finally, we should implement an adaptive tuning for optimal n_{kde} based on the acceptance rate.

-
- [1] K. Aggarwal et al. The NANOGrav 11 yr data set: Limits on gravitational waves from individual supermassive black hole binaries. *The Astrophysical Journal*, 880(2):116, jul 2019.
 - [2] Yves F. Atchadé and Jeffrey S. Rosenthal. On adaptive Markov chain Monte Carlo algorithms. *Bernoulli*, 11(5):815 – 828, 2005.
 - [3] Radu Craiu, Jeffrey Rosenthal, and Chao Yang. Learn from thy neighbor: Parallel-chain and regional adaptive mcmc. *Journal of the American Statistical Association*, 104:1454–1466, 12 2009.
 - [4] David J. Earl and Michael W. Deem. Parallel tempering: Theory, applications, and new perspectives. *Physical Chemistry Chemical Physics*, 7(23):3910, 2005.
 - [5] J. A. Ellis. A Bayesian analysis pipeline for continuous GW sources in the PTA band. *Classical and Quantum Gravity*, 30(22):224004, November 2013.
 - [6] Justin Ellis and Rutger van Haasteren. jellis18/ptmcmcsampler: Official release, oct 2017.
 - [7] Justin A. Ellis, Michele Vallisneri, Stephen R. Taylor, and Paul T. Baker. ENTERPRISE: Enhanced Numerical Toolbox Enabling a Robust Pulsar Inference Suite. Zenodo, sep 2020.
 - [8] A. Gelman, W. R. Gilks, and G. O. Roberts. Weak convergence and optimal scaling of random walk metropolis algorithms. *The Annals of Applied Probability*, 7(1):110 – 120, 1997.

- [9] Andrew Gelman and Donald B. Rubin. Inference from Iterative Simulation Using Multiple Sequences. *Statistical Science*, 7(4):457 – 472, 1992.
- [10] Heikki Haario, Eero Saksman, and Johanna Tamminen. An adaptive metropolis algorithm. *Bernoulli*, 7, 04 2001.
- [11] W. K. Hastings. Monte carlo sampling methods using markov chains and their applications. *Biometrika*, 57(1):97–109, 1970.
- [12] S. Hee, W. J. Handley, M. P. Hobson, and A. N. Lasenby. Bayesian model selection without evidences: application to the dark energy equation-of-state. *Mon. Not. Roy. Astron. Soc.*, 455(3):2461–2473, January 2016.
- [13] David W. Hogg and Daniel Foreman-Mackey. Data analysis recipes: Using markov chain monte carlo. *The Astrophysical Journal Supplement Series*, 236(1):11, may 2018.
- [14] Cajo J.F. Ter Braak Jasper A. Vrugt. Differential Evolution Markov Chain with snooker updater and fewer chains. *Statistics and Computing*, 18(4):435–446, 10 2008.
- [15] Yi Jin, Yulin He, and Defa Huang. An improved variable kernel density estimator based on l2 regularization. *Mathematics*, 9(16), 2021.
- [16] S. Kullback and R. A. Leibler. On Information and Sufficiency. *The Annals of Mathematical Statistics*, 22(1):79 – 86, 1951.
- [17] Tyson B. Littenberg. A detection pipeline for galactic binaries in LISA data. *Phys. Rev. D*, 84:063009, 2011.
- [18] J. B. MacQueen. Some methods for classification and analysis of multivariate observations. In L. M. Le Cam and J. Neyman, editors, *Proc. of the fifth Berkeley Symposium on Mathematical Statistics and Probability*, volume 1, pages 281–297. University of California Press, 1967.
- [19] Radford M. Neal. Slice sampling. *The Annals of Statistics*, 31(3):705 – 767, 2003.
- [20] Frank Nielsen. On the jensen–shannon symmetrization of distances relying on abstract means. *Entropy*, 21(5), 2019.
- [21] Emanuel Parzen. On Estimation of a Probability Density Function and Mode. *The Annals of Mathematical Statistics*, 33(3):1065 – 1076, 1962.
- [22] B. B. P. Perera et al. The International Pulsar Timing Array: Second data release. *Mon. Not. Roy. Astron. Soc.*, 490(4):4666–4687, 2019.
- [23] Gareth Roberts and Jeffrey Rosenthal. Examples of adaptive mcmc. *Journal of Computational and Graphical Statistics - J COMPUT GRAPH STAT*, 18, 06 2009.
- [24] Murray Rosenblatt. Remarks on Some Nonparametric Estimates of a Density Function. *The Annals of Mathematical Statistics*, 27(3):832 – 837, 1956.
- [25] David Scott and Stephan Sain. Multi-dimensional density estimation. *Data Mining and Data Visualization*, 24, 01 2005.
- [26] Stephen R. Taylor, Paul T. Baker, Jeffrey S. Hazboun, Joseph Simon, and Sarah J. Vigeland. enterprise extensions, 2021. v2.3.3.
- [27] Cajo J. F. Ter Braak. A Markov Chain Monte Carlo version of the genetic algorithm Differential Evolution: easy Bayesian computing for real parameter spaces. *Statistics and Computing*, 16(3):239–249, September 2006.
- [28] George R. Terrell and David W. Scott. Variable Kernel Density Estimation. *The Annals of Statistics*, 20(3):1236 – 1265, 1992.
- [29] W. D. Voudsen, W. M. Farr, and I. Mandel. Dynamic temperature selection for parallel tempering in Markov chain Monte Carlo simulations. *mnras*, 455(2):1919–1937, January 2016.

Appendix A: Kullback-Leibler divergence

We test the quality of our KDE by computing the KL divergence for each subgroup $\hat{f}_\alpha(\mathbf{x}_\alpha, \vec{h}_\alpha)$. Because we cannot know the true pdf for a set of samples $\{\vec{X}\}$, we have to resort to binning. From sub-KDE $\hat{f}_\alpha(\mathbf{x}_\alpha, \vec{h}_\alpha)$ built on subgroup of parameter samples $\{\vec{X}_\alpha\}$, we draw a new set of samples $\{\vec{X}_\alpha^*\}$. We estimate the corresponding normalized histogram distributions P_α and P_α^* using same grid of N bins to compute the KL divergence as [16] :

$$\text{KL}(P_\alpha \| P_\alpha^*) = \sum_{i=0}^N P_{\alpha,i} \left(\ln P_{\alpha,i} - \ln P_{\alpha,i}^* \right). \quad (\text{A1})$$

To avoid divergence of the logarithms, we set every $P_{\alpha,i}$ and $P_{\alpha,i}^*$ that are equal to 0 to the minimum found value in $P_\alpha \cup P_\alpha^*$ that is not 0.

Appendix B: Optimal bandwidth of KDE

We start this appendix with defining few useful expressions that will be used in our derivations later.

- The overlap between two neighbouring kernels of same bandwidth is given by

$$\int d\mathbf{x} K(\mathbf{x} - \vec{X}_a, \vec{h}) K(\mathbf{x} - \vec{X}_b, \vec{h}) = \prod_{i=1}^d \frac{\exp -\frac{1}{4} \frac{|\vec{X}_a - \vec{X}_b|_i^2}{h_i^2}}{\sqrt{\pi} 2 h_i}. \quad (\text{B1})$$

Let us remind you that d is the dimensionality.

- If a set of samples $\{\vec{X}\}$ of size N drawn from the probability density function $f(x)$, then we can approximate the averaging integral as :

$$\int dx f(x) g(x) \simeq \frac{1}{N} \sum_a g(X_a), \quad (\text{B2})$$

where the function g is evaluated at the sample points \vec{X}_a .

The main objective of this Appendix is to derive the optimal local bandwidth which is defined through the minimization of the mean square error:

$$\begin{aligned} \epsilon^2 &= \int dx (\hat{f}(x, h) - f(x))^2 \\ &= \int dx \hat{f}^2(x, h) - 2 \int dx \hat{f}(x, h) f(x) + \int dx f^2(x) \quad (\text{B3}) \\ &= \int dx \hat{f}^2(x, h) - 2 \int dx \hat{f}(x, h) f(x) + \text{const}, \end{aligned}$$

where $f(x)$ is the true PDF, $(\hat{f}(x, h))$ is its KDE approximation and $const$ is the term independent of the bandwidth h . We introduce local bandwidth h_a attached to each sample point X_a . Next we assume that all points in the vicinity of each point have similar bandwidth, in other words, $h_b \approx h_a$ for k_{near} local points X_b . Using these assumptions we can approximate the first term:

$$N^2 \int dx \hat{f}(x, h_a) \hat{f}x, h_b = \sum_a \prod_{i=1}^d \frac{1}{2\sqrt{\pi}h_{a,i}} + \sum_a \sum_{b \neq a} \prod_{i=1}^d \frac{e^{-\frac{1}{4} \frac{\Delta X_{ab,i}^2}{h_{a,i}^2}}}{2\sqrt{\pi}h_{a,i}}, \quad (B4)$$

where $h_{a,i}$ is i -th component of bandwidth attached to Gaussian kernel at \vec{X}_a and $\Delta X_{ab,i} = (\vec{X}_a - \vec{X}_b)_i$ is i -th component of the a vector connecting two samples in the parameter space.

Using now second bullet equation and excluding the actual sample from the sum (for improving stability and removing the possible bias, see "leave one out estimator" [15]) we obtain for the second term

$$2 \int dx \hat{f}(x, h_a) \hat{f}x \approx \frac{2}{N^2} \sum_a \sum_{b \neq a} \prod_{i=1}^d \frac{e^{-\frac{1}{2} \frac{\Delta X_{ab,i}^2}{h_{a,i}^2}}}{\sqrt{2\pi}h_{a,i}}, \quad (B5)$$

where we have assumed $N \gg 1$, $N(N-1) \approx N^2$. Combining these terms together gives us

$$N^2(\epsilon^2 - const) = \sum_a \left\{ \prod_{i=1}^d \frac{1}{2\sqrt{\pi}h_{a,i}} + \sum_{b \neq a} \prod_{i=1}^d \frac{e^{-\frac{1}{4} \frac{\Delta X_{ab,i}^2}{h_{a,i}^2}}}{2\sqrt{\pi}h_{a,i}} - 2 \sum_{b \neq a} \prod_{i=1}^d \frac{e^{-\frac{1}{2} \frac{\Delta X_{ab,i}^2}{h_{a,i}^2}}}{\sqrt{2\pi}h_{a,i}} \right\}.$$

Find the minimum of this expression by differentiating with respect to $h_{c,j}$ and equating it to zero:

$$0 = -\frac{1}{h_{c,j}} \prod_{i=1}^d \frac{1}{2\sqrt{\pi}h_{c,i}} \left\{ 1 + \sum_{b \neq c} \left[1 - \frac{1}{2} \frac{\Delta X_{bc,j}^2}{h_{c,j}^2} \right] \prod_{i=1}^d e^{-\frac{1}{4} \frac{\Delta X_{bc,i}^2}{h_{c,i}^2}} - 2(\sqrt{2})^d \left[1 - \frac{\Delta X_{bc,j}^2}{h_{c,j}^2} \right] \prod_{i=1}^d e^{-\frac{1}{2} \frac{\Delta X_{bc,i}^2}{h_{c,i}^2}} \right\}$$

Next we assume quite conservative approximation: $\frac{\Delta X_{bc,j}^2}{h_{c,j}^2} \ll$

1 for all points \vec{X}_b in vicinity of \vec{X}_c and all components j . This assumption overestimates the bandwidth and therefore conservative: this is what is used in this paper. Expanding in this small parameters and retain only the terms quadratic in this small ratio we obtain the system of linear equations for $1/h_{c,j}^2$:

$$\frac{k_{near}(2^{d/2+1} - 1) - 1}{(2^{d/2} - 1)} = \sum_{b \neq c} \left[3 \frac{\Delta X_{bc,j}^2}{h_{c,j}^2} + \sum_{i \neq j} \frac{\Delta X_{bc,i}^2}{h_{c,i}^2} \right]. \quad (B6)$$

Solving this system at each point \vec{X}_c for each direction in the parameter space (j) gives us the desired local bandwidth \vec{h}_c .

As an alternative approach we can assume that the bandwidth is comparable to the distance to the neighbours and define $h_{c,j}^2 = \Delta X_{c,j}^2(1 + \epsilon_{c,j})$, where $\Delta X_{c,j}^2 = 1/k_{near} \sum_b \Delta X_{bc,j}^2$ is the average square distance (i -th component) to the points in vicinity of \vec{X}_c and assume that $\Delta X_{bc,j}^2/\Delta X_{c,j}^2 \sim 1$ and $\epsilon_{c,j} \ll 1$ for all b, c, j . This yields

$$\prod_{i=1}^d e^{-\frac{1}{4} \frac{\Delta X_{bc,i}^2}{h_{c,i}^2}} \approx \left(1 + \frac{1}{4} \sum_i \frac{\Delta X_{bc,i}^2}{\Delta X_{c,i}^2} \right) \prod_{i=1}^d e^{-\frac{1}{4} \frac{\Delta X_{bc,i}^2}{\Delta X_{c,i}^2}}. \quad (B7)$$

Using this approximation we arrive at the system of linear equations for $1/h_{c,j}^2$:

$$-1 + \sum_{b \neq c} 2(\sqrt{2})^d \prod_{i=1}^d e^{-\frac{1}{2} \frac{\Delta X_{bc,i}^2}{\Delta X_{c,i}^2}} - P_{bc} \left(1 - \frac{1}{2} \sum_i \frac{\Delta X_{bc,i}^2}{\Delta X_{c,i}^2} \right) = \sum_{b \neq c} P_{bc} \left(3 \frac{\Delta X_{bc,j}^2}{\Delta X_{c,j}^2} \epsilon_{c,j} + \sum_{i \neq j} \frac{\Delta X_{bc,i}^2}{\Delta X_{c,i}^2} \epsilon_{c,i} \right),$$

where

$$P_{bc} \equiv \frac{1}{4} \left[\prod_{i=1}^d e^{-\frac{1}{4} \frac{\Delta X_{bc,i}^2}{\Delta X_{c,i}^2}} - 4(\sqrt{2})^d \prod_{i=1}^d e^{-\frac{1}{2} \frac{\Delta X_{bc,i}^2}{\Delta X_{c,i}^2}} \right].$$

Solving this system at each point \vec{X}_c for each direction in the parameter space (j) gives us the desired local bandwidth \vec{h}_c .

Appendix C: The M3C2 sampler

The M3C2³ (Multiple parallel Markov Chain Monte Carlo) is a python implementation of MCMC sampler. The aim of this tool is to improve the sampling robustness of complex posterior distribution, by running multiple chains in parallel. The cross check of the chain performance informs us about convergence (using Gelman-Rubin ratio [9]). We have implemented two mechanisms of building the chain (1) using slice sampling (`slice`) and (2) Metropolis-Hastings algorithm (MH) which could be used separately or together improving the mixture of the chains and reducing the auto-correlation length. Even though the sampler is very generic, we primarily use it within the context of GW data analysis. For the Metropolis-Hastings method we have implemented a set of proposal jumps:

- SCAM (Single Component Adaptive Metropolis), jumps along one randomly chosen direction given by the eigen vectors of the covariance matrix [10, 23]
- DE (Differential Evolution), jumps along the direction given by difference of two randomly chosen samples of the chains, or (as in the classic implementation [14, 27]) by using state of different chains running in parallel.
- ReMHA (Regional Metropolis Hastings Algorithm), the proposal represented by a mixture of several Gaussians distributions [3, 23].

For SCAM we build the covariance matrix adaptively based on the accumulated samples. The use of the accumulated samples breaks the Markov property of the chain, making it asymptotically Markovian. The stability of the covariance

matrix is yet another sign of the converged chain. One can stop adaptation after burn-in run. This proposal is suggested in [5].

ReMHA is similarly used adaptively. We use accumulated samples during the burn-in to estimate the number of clusters using Variational Bayesian Gaussian Mixture (`skikit-learn` package) and use this Gaussian mixture probability as a proposal. This proposal is somewhat similar to the one suggested in [3].

DE could be used as a proposal (snooker) described in [14] using multiple chains running in parallel or using the accumulated samples for each chain to propose the jump. There is no much difference between those two ways in case of well converged chains. However, the behavior and efficiency of those two implementations is very during the burn-in stage.

In slice sampling, we use slicing of the parameter space either randomly or along the eigen directions of the covariance matrix, the choice is made with a probability set by user. In case of mixture of `slice` and MH, the frequency of each method is defined by a user specified weight. In addition to preset proposals available in M3C2, user can add custom jump-proposals using a common interface. The weights and proposals can be set individually for each running chain.

Besides running parallel independent chains, M3C2 sampler has also parallel tempering implementation with an adaptive temperature ladder following [29]. The adaptation is aiming at increasing the acceptance rate between the chains.

The multi-chain scheme of M3C2 can be easily deployed on the multicore CPU infrastructure. Data exchange between chains, in case of parallel tempering, is restricted to its minimum level (pairwise communication between the chains), to ensure a good scalability.

³ <https://gitlab.in2p3.fr/lisa-apc/mc3>